Aalto University
School of Electrical Engineering

Effect of solar wind speed and IMF fluctuations on activity indices

Tuija I. Pulkkinen, Andrew Dimmock, Adnane Osmane, Reza Naderpour
Aalto University, Department of Radio Science and Engineering, Espoo, Finland

Katariina Nykyri
Embry Riddle Aeronautical University, Daytona Beach, FL, USA

Solar wind driver functions

Electric field

- Reconnection rate in antiparallel reconnection
- (*Burton et al., 1975*)

$$E_Y = -VB_Z$$

Epsilon

- Incident Poynting flux at magnetopause
- (*Akasofu, 1981*)

$$\epsilon = 10^7 l_0^2 V B^2 \sin^4(\frac{\theta}{2})$$

Universal coupling function

- Merging rate at magnetopause
- (*Newell et al., 2007*)

$$\left(\frac{d\phi}{dt}\right)^{3/4} = V B_T^{1/2} \sin^2(\frac{\theta}{2})$$

Parallel E-field

- Electric field along large-scale X-line
- (*Pulkkinen et al., 2010*)

$$E_{PAR} = VB\sin(\frac{\theta}{2})$$

Solar wind driver functions

Primary driver variables

- **Solar wind speed**
- **Interplanetary magnetic field (IMF) magnitude and orientation**

Driver properties

- Separation of variables
  $F(\mathbf{B}, V) = \mathbf{f}(V)\ \mathbf{g}(\mathbf{B})$
- Mean + fluctuation term
  $\mathbf{f}(V) = \langle \mathbf{f}(V) \rangle + \delta \mathbf{f}(V)$
  $g(\mathbf{B}) = \langle g(\mathbf{B}) \rangle + \delta g(\mathbf{B})$

$$E_Y = -V B_Z$$

$$\epsilon = 10^7 l_0^2 V B^2 \sin^4\left(\frac{\theta}{2}\right)$$

$$\left(\frac{d\phi}{dt}\right)^{3/4} = V B_T^{1/2} \sin^2\left(\frac{\theta}{2}\right)$$

$$E_{PAR} = V B \sin\left(\frac{\theta}{2}\right)$$

Higher *V* produces stronger *AL*

$$E_Y = -V B_Z$$

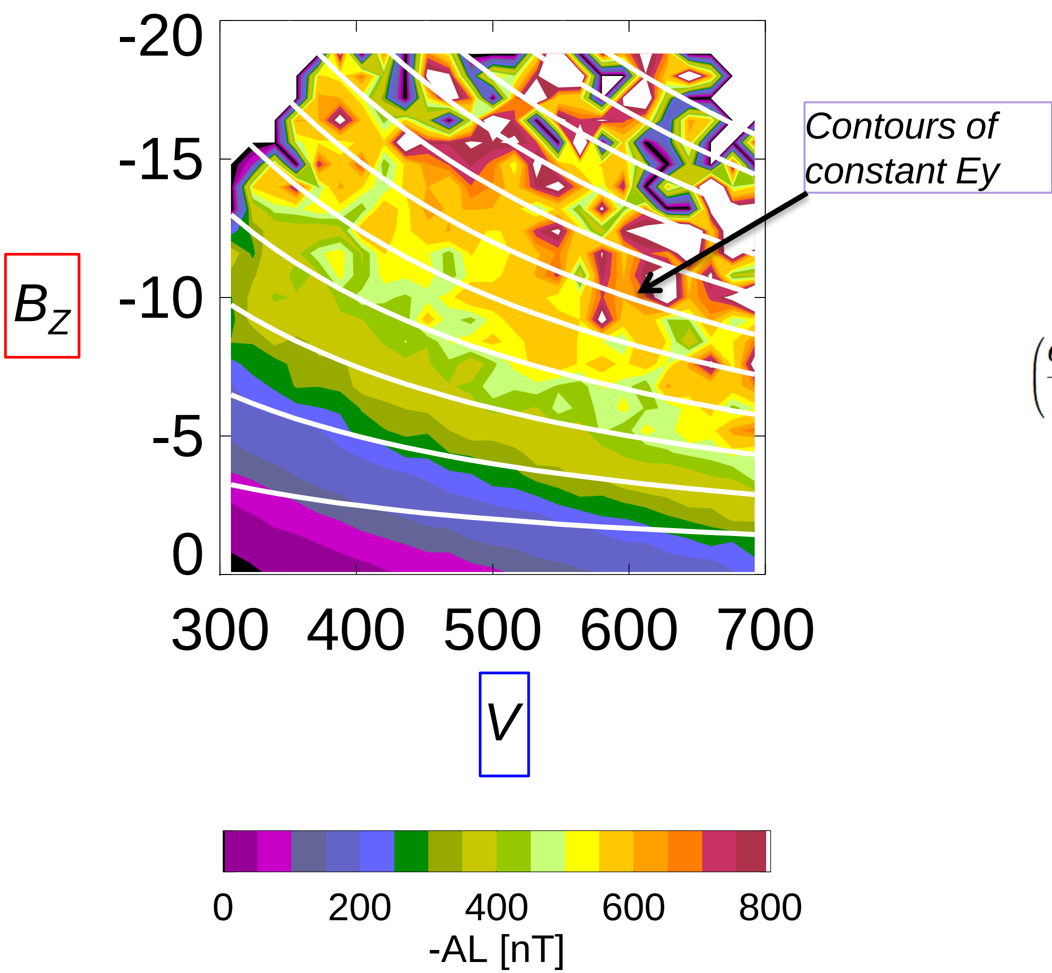

$$\epsilon = 10^7 l_0^2 V B^2 \sin^4(\frac{\theta}{2})$$

$$\left(\frac{d\phi}{dt}\right)^{3/4} = V B_T^{1/2} \sin^2(\frac{\theta}{2})$$

$$E_{PAR} = V B \sin(\frac{\theta}{2})$$

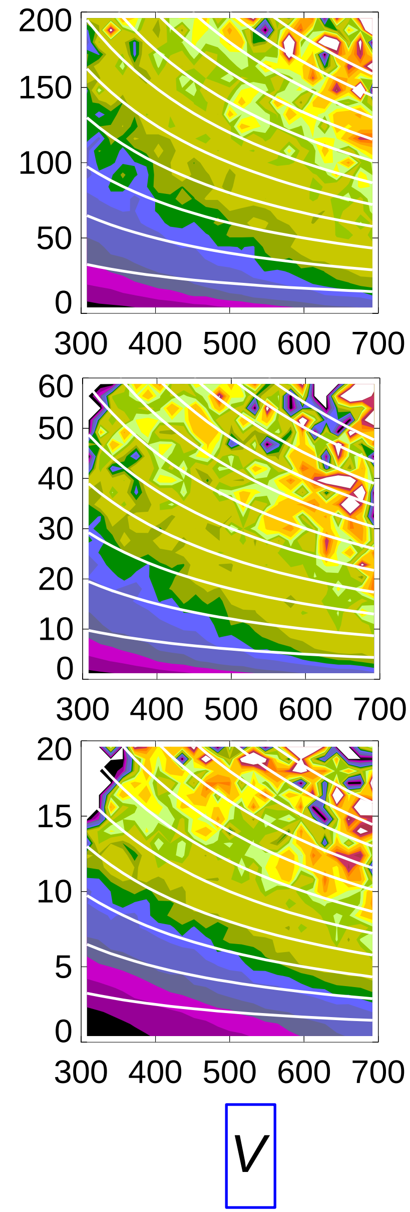

OMNI hourly averages 1963-2013

Themis statistical analysis

Shock – magnetosheath coordinate system

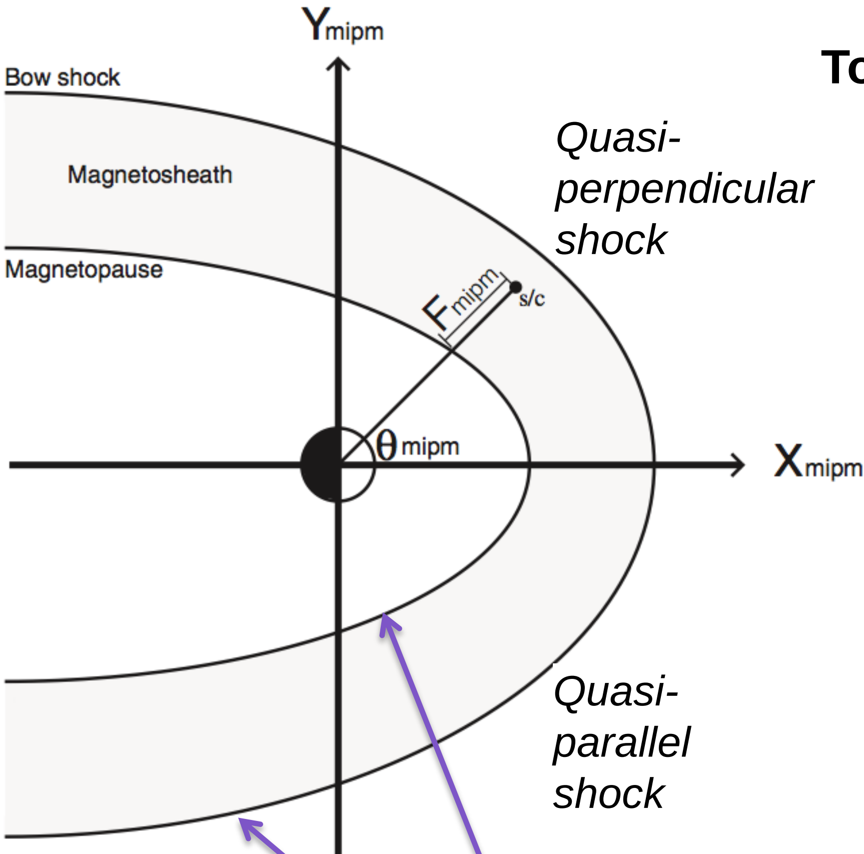

Tool to organize data with respect to

- upstream conditions and
- magnetospheric boundaries

$$\hat{e}_x = -\frac{\mathbf{V}}{|\,\mathbf{V}\,|}$$

$$\hat{e}_y = -sign(\mathbf{B}\cdot\hat{e}_x)\frac{\mathbf{B} - B_{\hat{e}_x}\hat{e}_x}{|\,\mathbf{B} - B_{\hat{e}_x}\hat{e}_x\,|}$$

$$\hat{e}_z = \hat{e}_x \times \hat{e}_y$$

Shue magnetopause model

Verigin bow shock model

(Dimmock et al., JGR 2013)

Plasma after shock crossing:
Electric field largest at quasi-parallel side

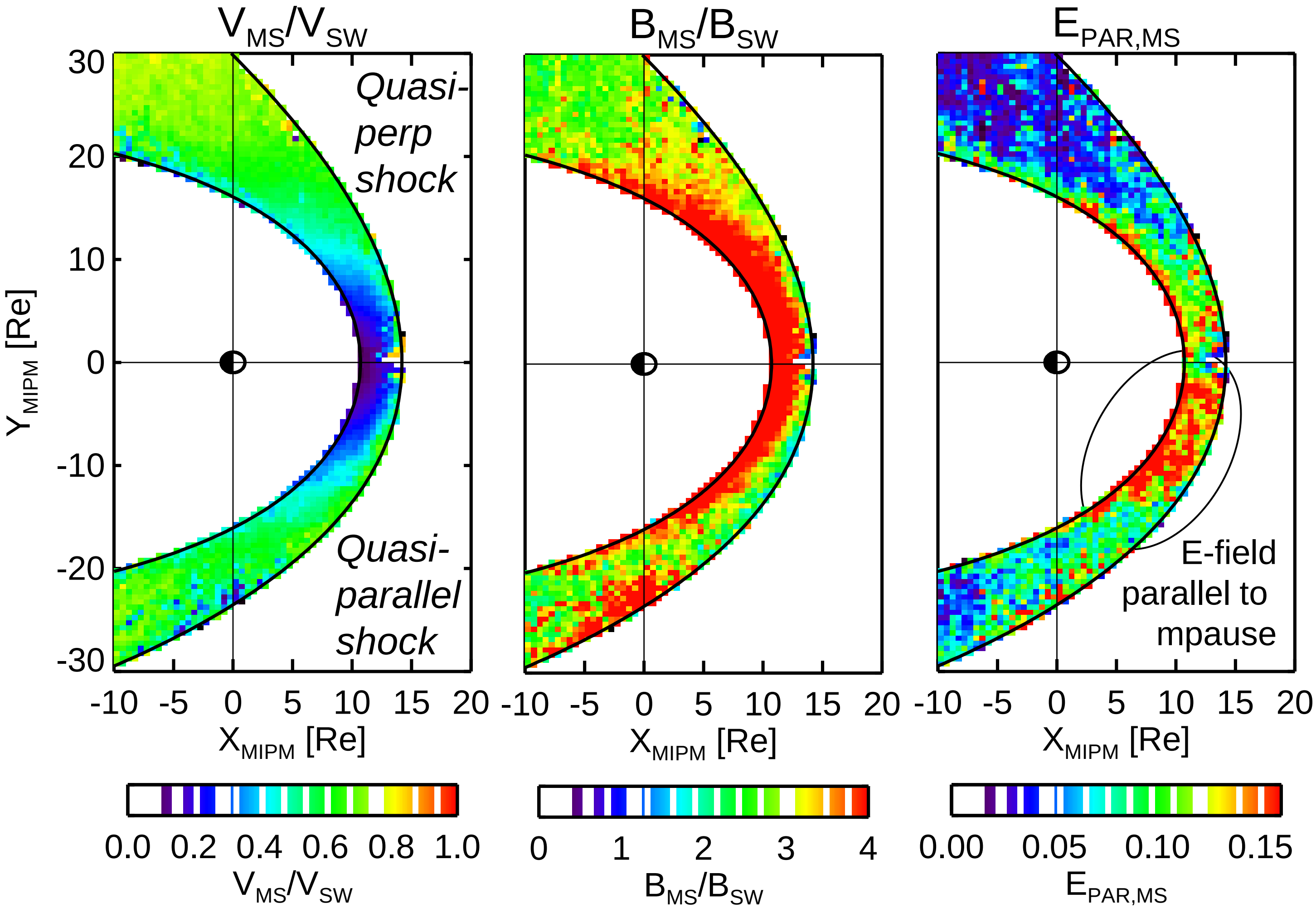

- **Speed** reduced at subsolar region
- **Magnetic field** enhanced at subsolar region
- **Electric field** parallel to magnetopause only a fraction of solar wind Ey

Themis statistical analysis

Plasma after shock crossing:
Examine different solar wind V, B -combinations

	Small E	Intermediate E		Strong E
V_{SW}	< 400	< 400	> 400	> 400
B_S	$-2.5 < B_Z < 0$	< –2.5	$-2.5 < B_Z < 0$	< –2.5
	slow V ***low*** B_S	***slow V*** ***large*** B_S	***fast V*** ***low*** B_S	***fast V*** ***large*** B_S

Only negative IMF B_Z observations included

Plasma after shock crossing:
Moderate driver with high V most efficient

Electric field parallel to magnetopause, scaled by upstream average

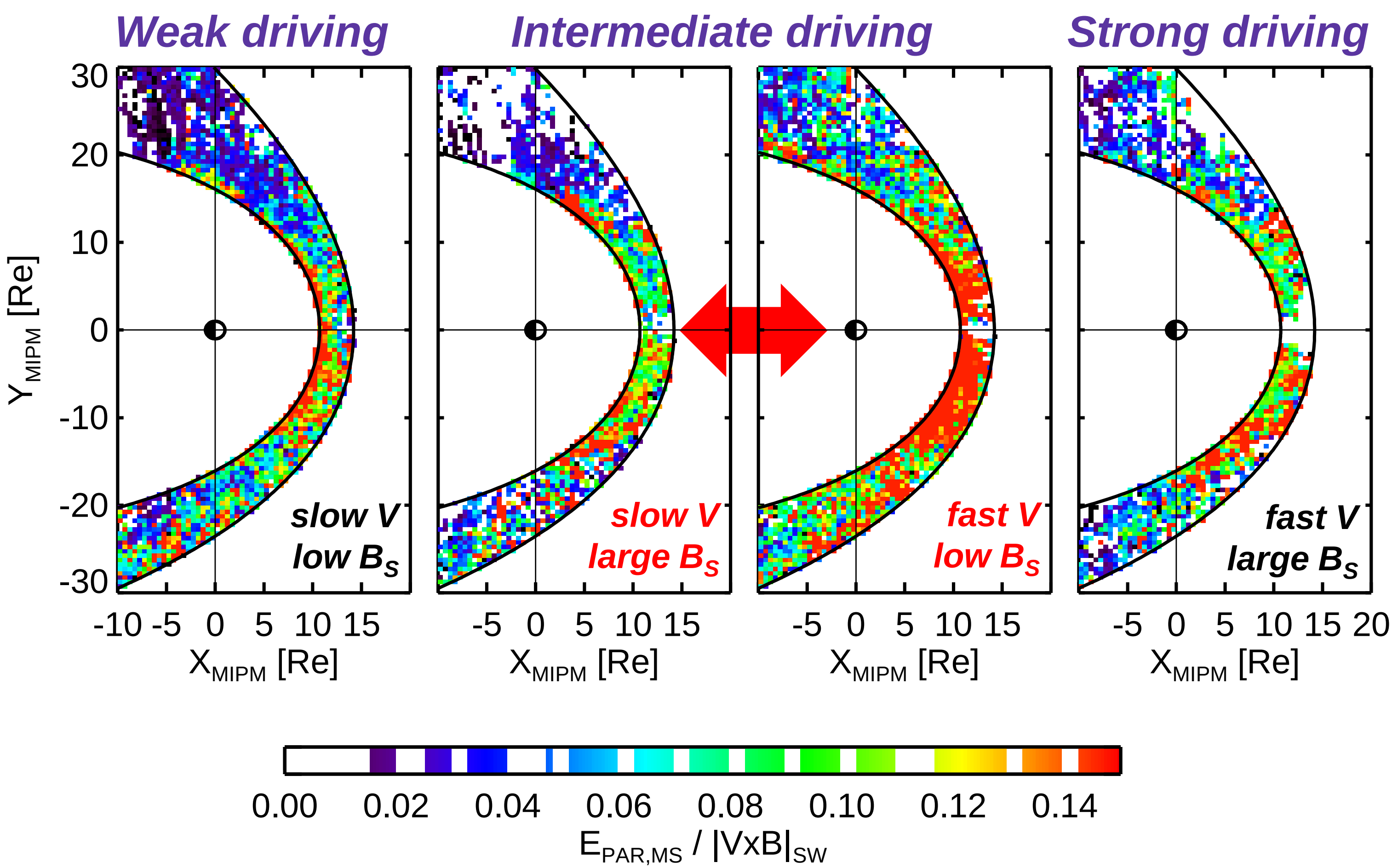

Themis statistical analysis

Plasma after shock crossing:
Moderate driver with high V most efficient

Poynting flux perp to magnetopause, scaled by upstream value

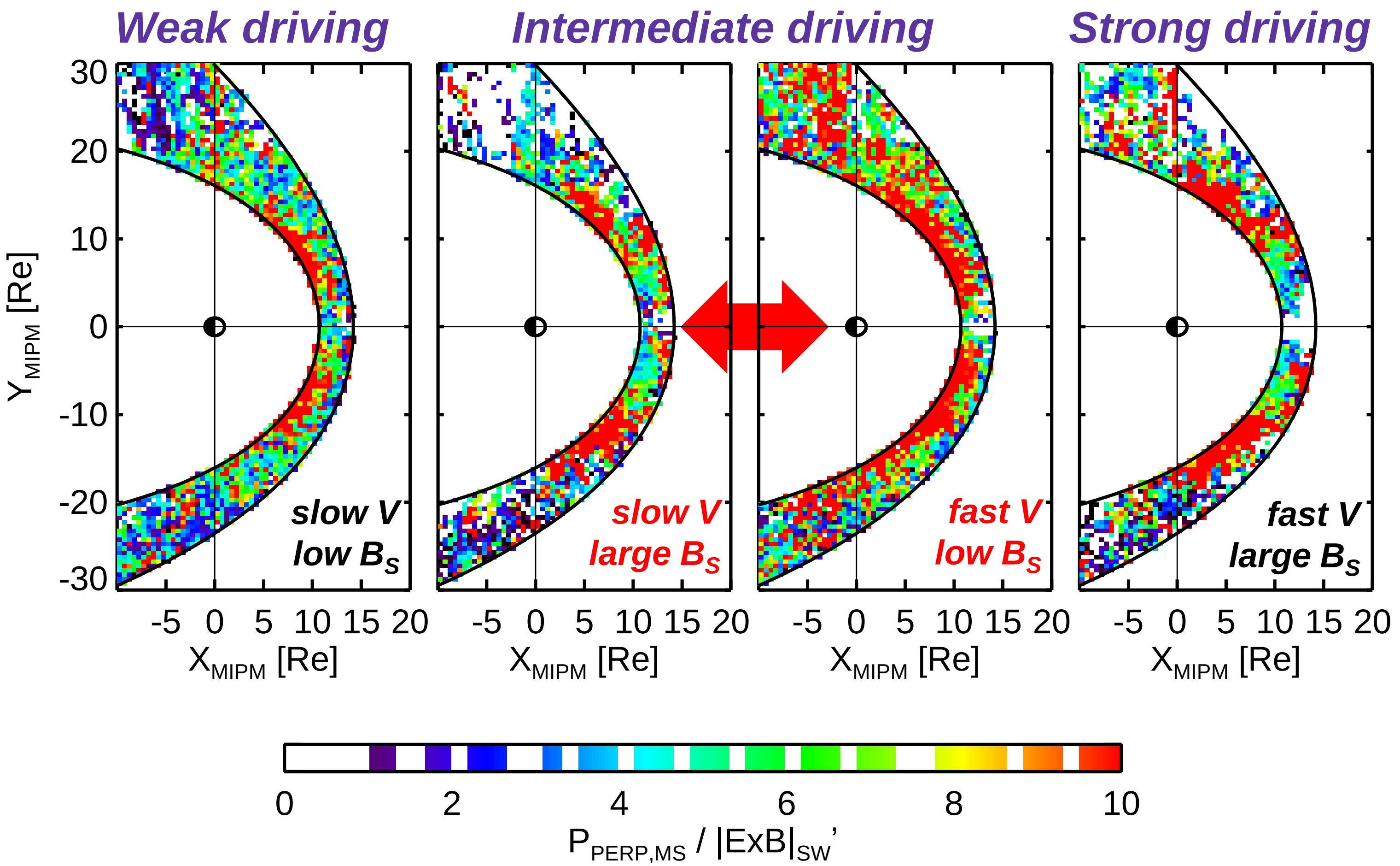

Themis statistical analysis

Scaled Values at the Magnetopause

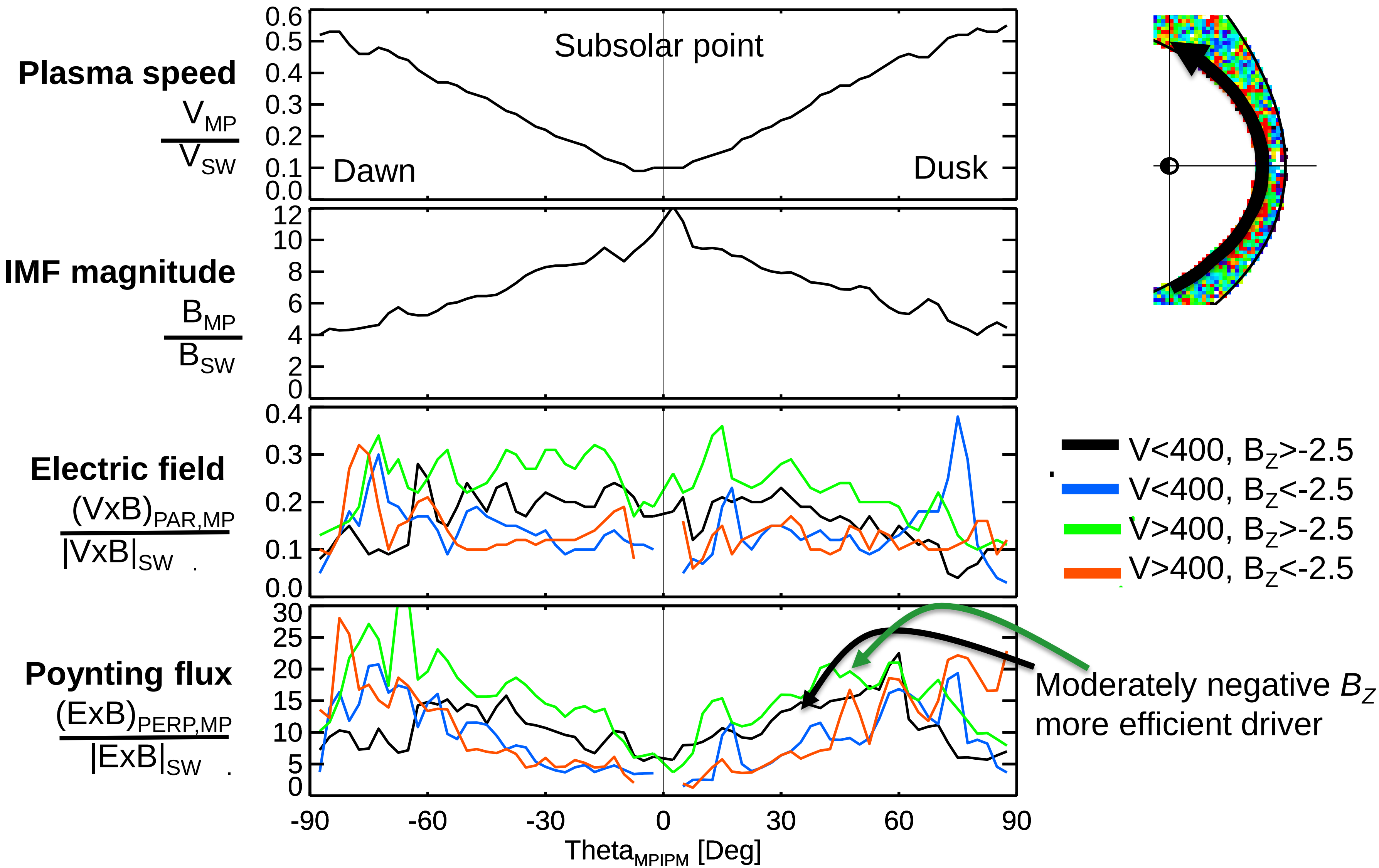

Higher variability produces higher AL

AL as function of solar wind electric field and speed variance

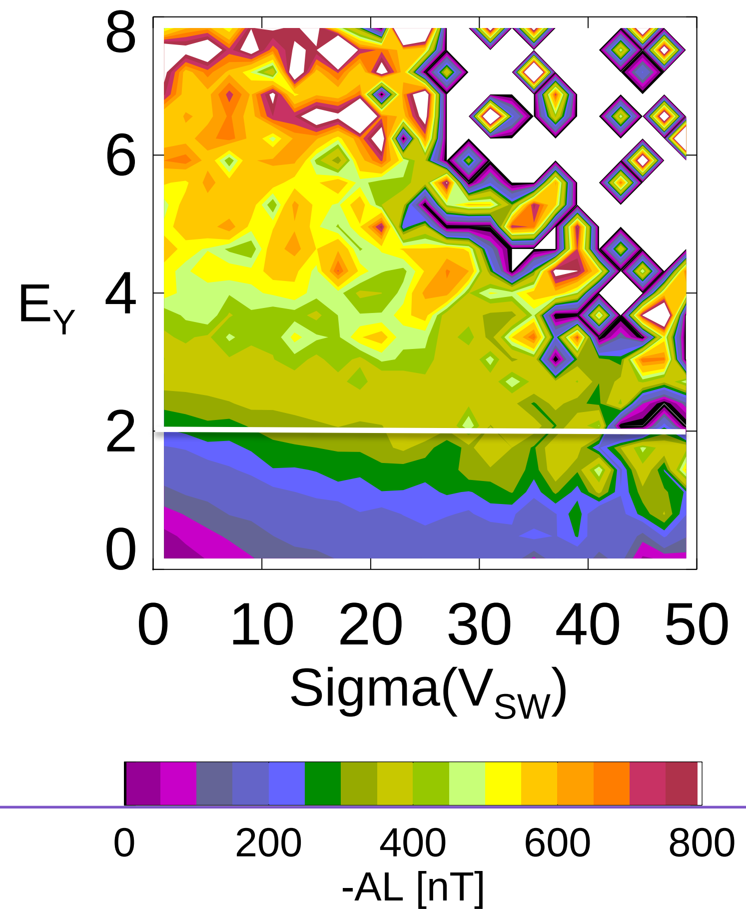

Aalto University
School of Electrical
Engineering

Hourly variances from OMNI dataset

Plasma after shock crossing:
Magnetosheath perpendicular velocity fluctuations

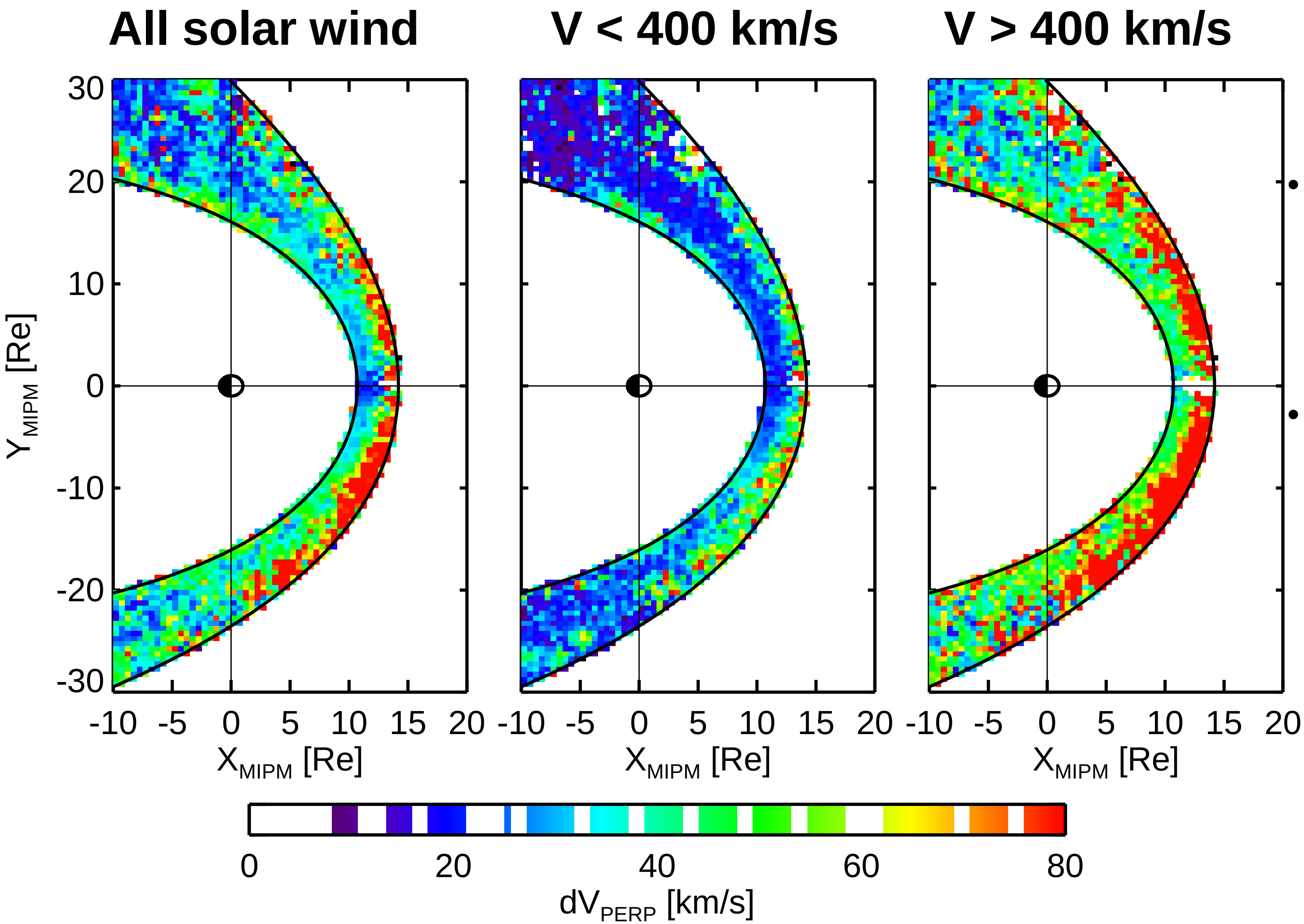

- Magnetosheath fluctuations larger for high solar wind speed
- High speed often implies high fluctuations in solar wind V

Themis observations 2007-2013

Local MHD simulations
Kelvin-Helmholz instability at magnetopause

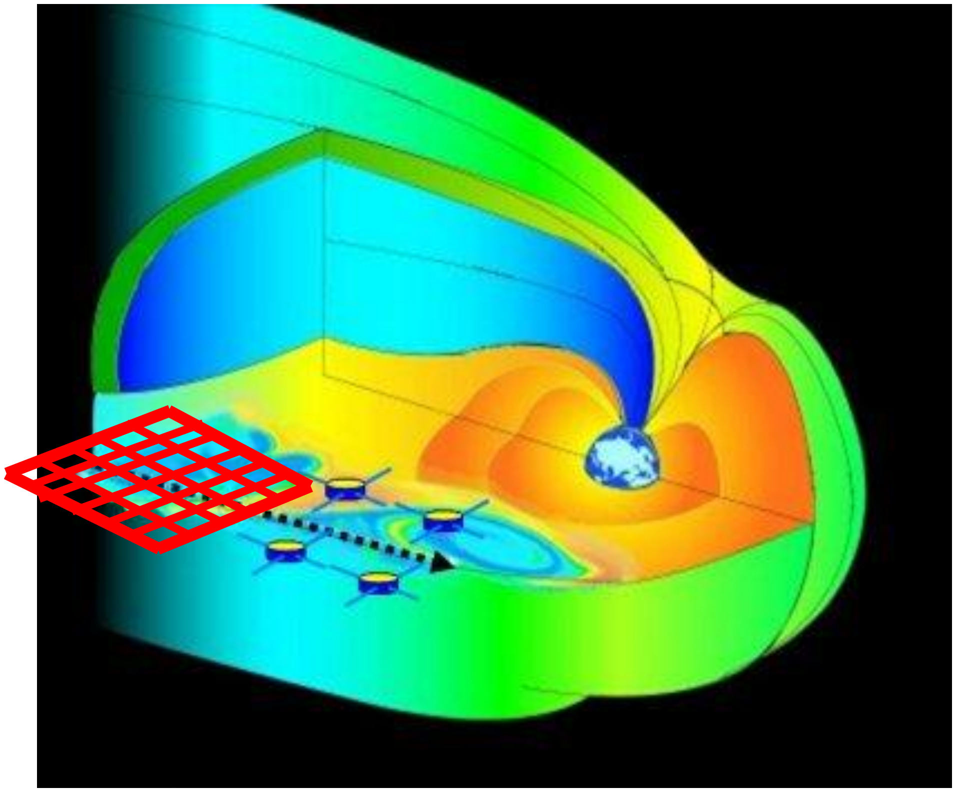

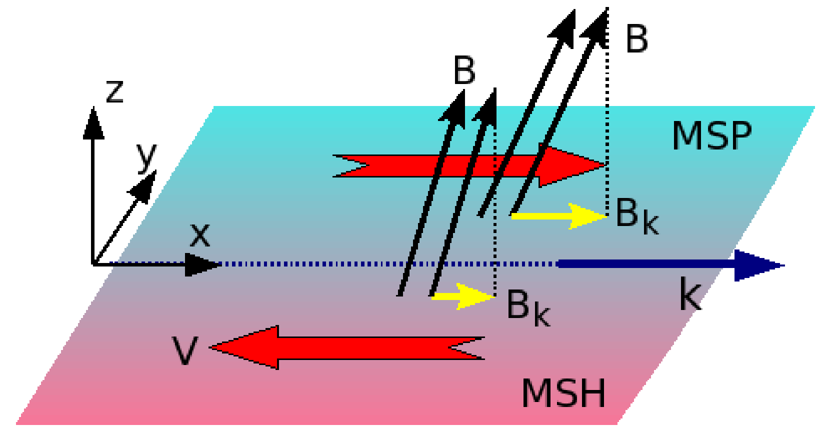

Onset condition for KHI

$$\frac{m_0 n_1 n_2}{n_1 + n_2}[\mathbf{k} \quad \Delta\mathbf{V}]^2 > \frac{1}{\quad_0}\left((\mathbf{k} \quad \mathbf{B}_1)^2 + (\mathbf{k} \quad \mathbf{B}_2)^2\right)$$

(e.g., Nykyri, 2013)

Magnetosheath fluctuations enhance reconnection and plasma transport

Magnetosheath fluctuations change KHI dynamics:

- timing of reconnection onset
- amount of reconnected material

Single mode analysis:

- Pc3-frequency range fluctuations produce plasma transport first

Multi-mode analysis (Pc2-Pc5):

- Non-linear interaction of modes affects KHI dynamics and reconnection timing

Plasma velocity and density

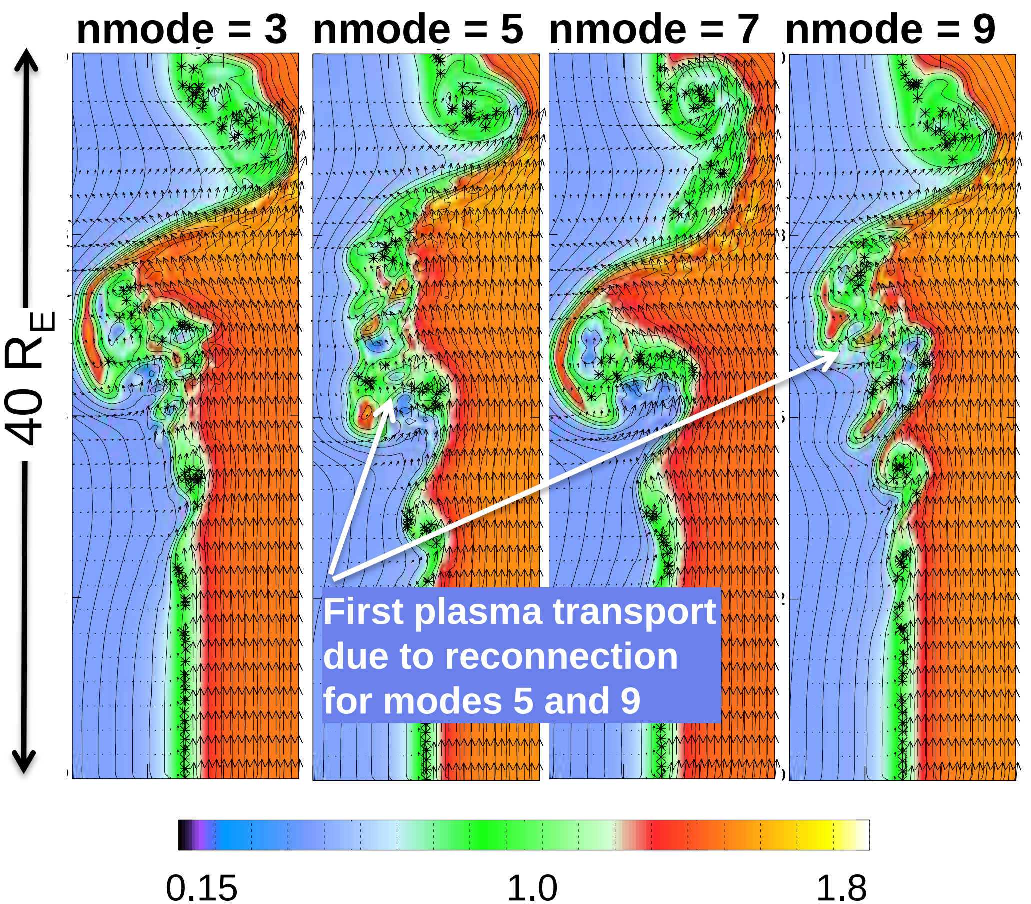

(Nykyri et al., 2014 in preparation)

OMNI statistical analysis:
Wavelet analysis of IMF fluctuations

Wavelet spectrum power integrated over range of frequencies

- 1-10 min -> ULF power
- 10-30 min -> lower frequency fluctuations

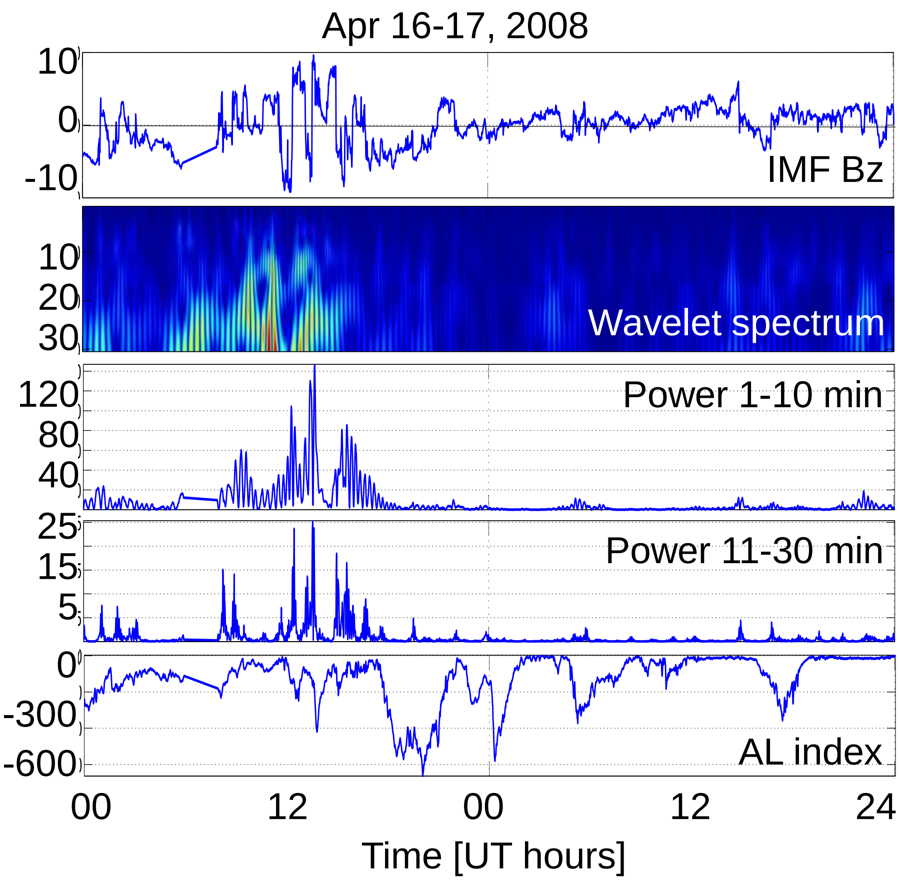

(Naderpour et al., 2014 in preparation)

ULF fluctuations in B_Z drive higher AL

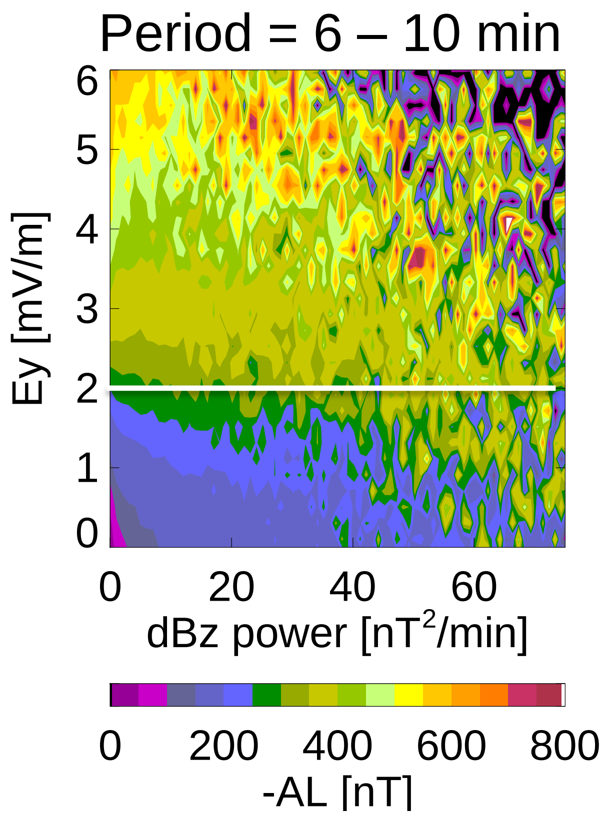

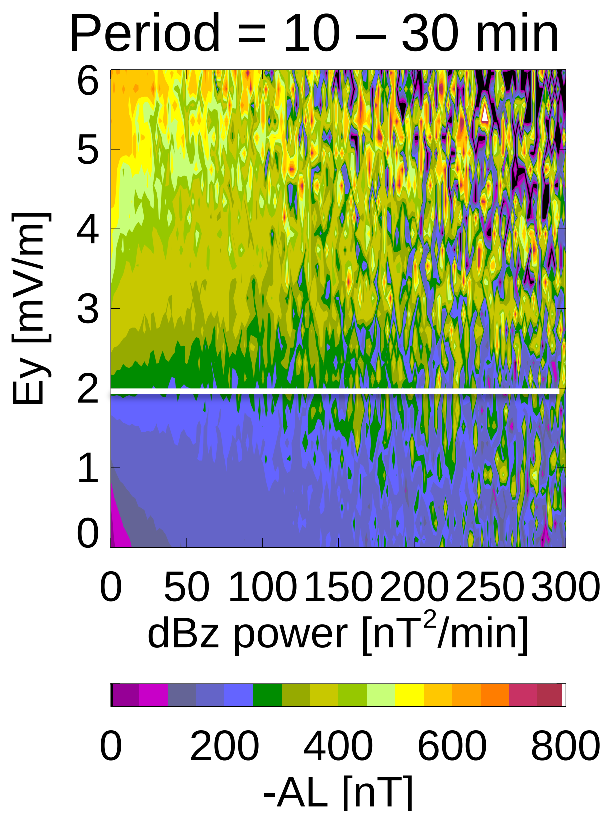

Wavelet analysis of 1-min OMNI data (Naderpour et al., 2014 in preparation)

Conclusions

1. For all driver functions, **higher V produces stronger AL** compared to similar value of driver function but with lower V
2. Electric field transport from solar wind to magnetosheath more efficient when **V is higher -> higher driver at magnetopause**
3. For all driver functions, **higher level of fluctuations produces stronger AL** compared to similar average with less fluctuations
4. **ULF waves** are especially **efficient in driving AL** activity
5. **Magnetosheath fluctuations** are **larger when V is higher**
6. **ULF waves drive KHI at magnetopause** which enhances **reconnection and plasma transport -> stronger AL**